Improvised convolutional auto encoder for thyroid nodule image enhancement and segmentation

Drakshaveni Gunjali[1], Prasad Naik Hamsavath[2]
[1]Department of Master of Computer Applications, BMS Institute of Technology and Management, Bangalore, India
[2]Department of Master of Computer Applications, NITTE Meenakshi Institute of Technology, Bangalore, India

Article Info

ABSTRACT

Thyroid ultrasonography and thermography are a widely used clinical technique for nodule diagnosis in thyroid regions. However, it remains difficult to detect and recognize the nodules due to low contrast, high noise, and diverse appearance of nodules. To alleviate doctors' tremendous labor in the diagnosis procedure, we advocate a machine learning approach to the detection and recognition tasks in this paper. Moreover, this research mainly focuses on segmenting the image and finding the probable region. In this research work an improvised convolutional auto encoder (ICAE) is introduced for segmenting the image and finding the probable region of thyroid gland and it enhances image. ICAE comprises various layer and mechanism, each having their own task. Apart from the traditional approach, skip connection is applied for the image enhancement and dual frame is introduced for better feature extraction. Further optimization technique is used for increasing the learning rate. ICAE is evaluated considering digital database thyroid image (DDTI) dataset with performance metrics like accuracy, true positive rate, false positive rate, dice coefficient and similarity index (SI); also, comparative analysis is carried out with various existing model and proposed model simply outperforms the existing model.

This is an open access article under the CC BY-SA license.

Corresponding Author:

Drakshaveni Gunjali
Department of Master of Computer Applications, BMS Institute of Technology and Management
Bangalore, India
Email: gdrakshaveni23@gmail.com

1. INTRODUCTION

In last decade, thyroid cancer growth has been unanimous and further growth rate is 4.5% i.e., higher than any other cancer [1]; moreover, in the year 2019, nearly 54,000 new thyroid cancer has been reported in the USA alone and nearly 2060 people passed away due to this. Furthermore, it is observed that chances of turning benign to malignant with a rate of 4.5%-6% [2]; hence several health task force recommends the screening of thyroid cancer which includes ultrasound and neck palpation in asymptomatic people [1]. However, screening process faces huge issues, this causes thyroid nodules to opt for a various method such as computed tomography, ultrasonography and magnetic resonance imaging (MRI); ultrasonography is one of the popular diagnostic tools as it is easily available and inexpensive. Ultrasonography not only differentiate among solid nodules consisting of cystic components, but it also deals with nodule pathology. Moreover, ultrasonography increases more indication of increased malignancy risk which includes microcalcification, extrathyroidal margins, wide nodules and hypoechoic solid nodules and further, it ignores round shape, cystic composition, smooth margins, spongiform appearance, and echogenicity that are associated with benign disease [3], [4].

In general, thyroid segmentation is carried into two directions [5], [6] i.e., thyroid nodule and thyroid gland segmentation [7], [8]; although both are almost same, further can be categorized in four distinctive part [9]-[13] i.e., shape and contour-based, region-based, hybrid approach, machine learning (ML) approach; these four methods are described as: i) Shape and contour-based approach: In this type of approach, shape or boundary is used as the gland or nodule information for segmentation of nodule or gland in ultrasound (US) image; in this case boundaries between nodule and tissue can be blurred due to image artefacts and image contrast. Further, thyroid nodules are considered to be irregular. Hence these mechanism requires prior information of contour and shape for improvisation inaccuracy. ii) Region-based method: In this approach, statistical properties between the regions are utilized, these include variance and mean to achieve minimum energy function; further this approach assumes that same tissue are considered to homogeneous and various regions are considered too inhomogeneous. However, in reality, it is ambiguous, thus this approach requires prior shape and spatial location information. iii) Deep learning (DL) and ML mechanism: In this approach construct classifier is used for classifying the image blocks or pixels in US image; these classifiers are mainly based on machine learning algorithm [12], [13] which includes convolutional neural network (CNN), decision tree (DT), radial basis-function neural network (RBFNN), feedforward neural network (FNN), support vector machine (SVM), extreme learning machine (ELM) and so on. However, it faces the problem of training which is time-consuming and requires huge training tags and data. iv) Hybrid approach: This approach integrates any of the two methods for improvising the segmentation; considering the segmentation, this is undoubtedly best method; however it gets more complex due to two different approach [14]-[19].

Motivation and contribution of research work. Thyroid nodules have various forms including predominantly cystic, predominantly solid, cystic, and solid; moreover, segmentation of cystic components inside given thyroid nodule identifies the nodule composition. Moreover, the cystic component might appear as the hypoechoic region in the ultrasound image and hypoechoic region might be the cystic therefore it should not be considered as veins or arteries outside the gland as both have a similar structure. Hence segmentation mechanism needs to design in such a way that at first thyroid gland has to be identified then cystic components needs to be identified inside the nodules [20]-[23]. Moreover, deep learning has various application in the medical field as it is fully automatic with interface time of milliseconds and do not require any kind of seed, this characteristic of deep learning domain makes the model for real-time adoption. In deep learning, CNN has been very popular for image processing; hence in this research work, we adopt the deep learning domain and adopt the convolution auto-encoder for segmentation and improvise it. A convolutional auto-encoder is a neural network architecture that can be customized following application; further contribution of the research work has been highlighted through below points:

At first, we perform extensive research of existing segmentation approach [24]-[29], study their methodologies and analyze their shortcoming. Further, we design and develop improvised convolution auto encoder aka (ICAE) for thyroid gland segmentation; ICAE not only helps in segmenting and finding return on investment (ROI) but also enhances the image. ICAE comprises various parts or layers; each layer has its significance. ICAE considers the denoising image through skip connections in the model and dual frame is introduced for better feature learning. Further global and local feature are learned and integrated to enhance the segmentation through edges; at last batch, normalization is introduced for increasing the higher learning rate. ICAE is evaluated considering various metrics with different existing methodology.

2. LITERATURE SURVEY

In this section of research work, the various existing model of segmentation is discussed, and their shortcomings are highlighted; although there exist plenty of methods, we focus on related existing mechanism. In the paper, Mahmood and Rusli [19] developed an integrated model of active contours without edges (ACWE) and geodesic/geometric contours (GC) and design a novel method for optimal segmentation. In here, at first energy function from inside and outside the contour are discretized through binary variable to mark the position in a given image, further contour length is discretized through geo-cuts approach, also these two methods were combined, and new energy function was introduced. Although this method improvises in terms of computing speed and prevents boundary leakage, it lacks quantitative performance and faces huge complexities. Moreover, sub-centimeter identified through ultrasound is not recommended in case of fine needle aspiration as it requires extra attention and cares for various parameters such as size estimation, volume estimation and nodule shape as this parameter have a huge role for the decision-making process of fine needle aspiration (FNA) biopsy. Segmentation of thyroid nodules helps in the estimation of the above parameter, segmentation is a major challenging task due to several reasons such as poor contrast among various anatomies and granular speckle; further considering the importance of segmentation, a significant amount of research has been carried out, this method includes radial basis FNN [5], active contour-based segmentation [6], optimized active contour [7], localized active contour [8], local region active

contour [9], geodesic level set [10], bilateral filtering [10] and hybrid model [11], extreme-ML [12] and random forest (RF) CNN model [11], [13] and few other research focused on manual segmentation. Moreover, it was observed that most existing mechanism of segmentation approach focuses on drawing manual boundary known as a seed which restricts the usage in a real-time scenario.

Apart from the above approach, last decade has seen a rise of deep learning concept in segmentation; moreover, it is observed that deep neural network (DNN) performs extremely well in object recognition, semantic segmentation and detection [30]-[33]. Hence [20] applied the CNN for segmenting the thyroid nodules in 2D images of thyroid; here proposed CNN comprises two max-pooling layers and 15 convolutional layers. Further, tenfold cross-validation is used for quantitative evaluation, out of these 10 folds eight were training and one for validation and residual one was for testing. Similarly, cascaded CNN was designed in [21] in consideration of the same architecture presented in [20]; CCNN mechanism comprises three distinctive phases for segmentation of thyroid nodule. At first, U-net architecture was used for ROI extraction which consists of a thyroid nodule, later artificial masks were designed through the manual process of boundary adjustment and sign recognition [22] considering the ultrasonic examinations for patients. Moreover, artificial masks were mainly focused on the right, left, the lower and upper part of thyroid nodule; however, due to manual process model efficiency puts a huge question of deployment in real-time [34]. Further, the above methods also fail to obtain the trade-off among complexity and various performance metrics.

3. PROPOSED METHODOLOGY

In this section we design and develop improvised convolutional auto encoder for image segmentation. The proposed mechanism comprises various mechanism and layer. First we consider the general convolutional auto encoder. Second apply skip connection for image enhancement. Later for feature learning we apply dual frame. Alongside to learn the higher rate we optimize it through batch normalization process. The modified convolutional auto encoder with skip connection will aid in achieving very good thyroid nodule segmentation outcomes.

3.1. Generalized convolutional auto encoder

Convolutional auto encoder comprises two important operations i.e., convolution and activation; these two are combined with the pooling operations. Convolution layers are responsible for generating the various features for minimizing the computational capacity through distributing the kernel coefficients for a particular feature map. Moreover, apart from general ICAE comprises various convolutional kernel in each layer. Moreover, activation function has similar role for the introduced filters after kernels, which in terms imposes network non-linearity. Furthermore, fully convolutional network aka, convolution with kernel and bias value is mathematically represented through (1).

$$a^g = \left\{ a_1^g, a_2^g, \ldots \ldots, a_{I_g}^g \right\}$$
$$u^g = \left\{ u_1^g, u_2^g, \ldots \ldots, u_{I_g}^g \right\} \tag{1}$$
$$z^g = \left\{ z_1^g, z_2^g, \ldots \ldots, z_{I_g}^g \right\}$$

Moreover, by considering the FCN, convolution with kernel and bias value activation function can be designed and computed through equation, also the activation is for the ith layer.

$$a^g \equiv A^g \left(B(a^{g-1}); \tau^g \right), 1 \le g \le j,$$
$$a_h^g = \eth \left(u_h^g \otimes B(a^{g-1}) + z_h^g \right) \in a^g, 1 \le g \le I_{g,} \tag{2}$$

In (2), $\otimes$ represents the convolutional operator, $\eth(.)$ represents the activation function and B indicates the down sampling; also τ^g represents the entire parameter for the given layer. Further pooling helps in handling the huge range of receptive field in global features, also it helps in minimizing the parameter. In ICAE mechanism, we consider parametric rectifier linear unit (PReLU) for activation; since ReLU provides huge advantage in deep learning and provides the efficient solution than the sigmoid function. The main advantage of PReLU is that it helps in learning the small value while training the model which, this further helps in adopting the better parameters such as biases and weights. In case of feed forward network, single slope parameter is learned in each layer whereas with this activation function it is possible for each channel in each layer. Moreover, the mathematical definition of this activation function is given as (3).

$$f(v) = \begin{cases} v & if \ v \ is \ greater \ than \ zero \\ (param)v & if \ v \ is \ less \ than \ or \ equal \ to \ zero \end{cases} \tag{3}$$

Moreover if $param$ is the learnable parameter then it is considered as the PreLu and modified mathematical definition can be given through (4).

$$e(v) \equiv \max(v, 0) + (param)min(0, w) \tag{4}$$

In (4), the parameter is indicated through $param$ and it ranges between 0 to 1. Moreover, feed forward of ICAE is represented as (5).

$$(G; \tau) = \tilde{A}^{2j-1} \begin{pmatrix} \cdots \dot{A}^{j+1} \left(A^j (\cdots A^2(G; \tau^1); \tau^2) \cdots; \tau^k \right); \\ \tau^{k+1}) \cdots; \tau^{2k-1} \end{pmatrix} \tag{5}$$

In (5), auto encoder mechanism G indicates the input which is equal to down sampling from (7). Set of parameters represented through (6).

$$\tau = \{\tau^1, \tau^2 \ldots \ldots \tau^{2j-1}\} \tag{6}$$

Convolutional layer output is computed through below equation where S indicates the up sampling with $\dot{A}^q$ indicating convolutional layer output to reconstruct the matrix.

$$\dot{a}^q = \dot{A}^q (S(\dot{a}^{p-1}); \delta^p), j + 1 \leq p \leq 2j - 1$$
$$\dot{a}_r^q = e\left(u_o^p \otimes S(\dot{a}^{p-1}) + z_o^p\right) \in \dot{a}^q, 1 \leq o \leq L_{p,} \tag{7}$$

Decoding part of convolutional auto encoder is computed in (10) where b^r indicates the set of bias value in given layer p. Moreover, reconstruction has the matrix of size given and convolutional kernel and bias is given in (8).

$$u^p = \left\{u_1^p, u_2^p, \ldots \ldots, u_{L_{p,}}^p\right\}$$
$$z^p = \left\{z_1^p, z_2^p, z_{L_{p,}}^p\right\} \tag{8}$$

Once the activation function is employed, we tend to improvise the learning rate by updating the set parameter in backpropagation. Moreover, learning rate is improvised through method of steepest descent where first order derivative is computed to find the local minimum and local maximum which further helps in reducing the loss function.

$$argmin_\tau E(A(G; \tau); M) \tag{9}$$

In the (9), M is output and E is loss function for measuring the error.

3.2. Image enhancement

The Figure 1 shows comparisons of generalized and proposed convolution auto-encoder. Moreover the general convolutional auto-encoder model as described in Figure 1(a) gives efficient result but it faces huge loss of information. This is overcome through introducing the skip connection in proposed model described in Figure 1(b) as it helps in improvising the information loss. Skip connection adds the local features to decoder. Furthermore indicates the proposed convolutional auto encoder with skip connection which is used for enhancing the image.

The standard generalized convolution auto-encoder passes complete feature data through representation and retain low resolution feature information only in next stage; further, spatial information of smaller object is lost because of resolution loss post pooling operation. On the other side the proposed convolutional auto encoder, for smaller object, without any information loss in pooling operation the global feature is retained. The spatial feature is retained through introduction of blocking deconvolution path. Similarly, for larger objects, the skip connection is primarily focused to extract edge feature information. In proposed convolutional auto encoder, the deconvolution and activation of residual path include feature set to the skip connection based on object size.
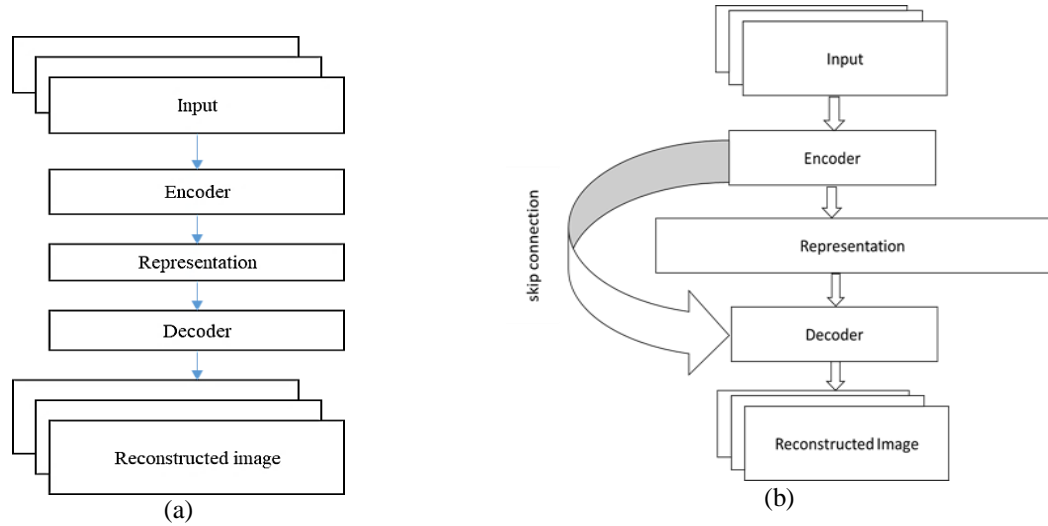
Figure 1. Comparizon of convolutional auto-encoder, (a) generalized convolutional auto-encoder without skip connection and (b) proposed convolutional auto-encoder with skip connection

Further we develop and design an improvised convolutional auto encoder aka ICAE; in here convolutional auto encoder is applied in recursive manner for low resolution; convolutional auto encoder with skip connection can be represented as in (10).

$$A = \mu^{trans} F_{param}(d) \varphi \tag{10}$$

In the (10), φ represents filters and μ^{trans} indicates the pooling operator and uses pooling average where low pass filtering is used; the (10) indicates the framelet coefficient of convolution. F_{param} indicates the hankle matrix which is responsible for the convolution; Since convolution auto encoder is bypass connection, it can be further represented as (11):

$$W = \begin{bmatrix} A \\ Q \end{bmatrix} = Y(d \circledast \varphi) \tag{11}$$

where each parameter is formulated through given in (12).

$$
\begin{aligned}
R &= \begin{bmatrix} I\_M \\ \mu^{trans} \end{bmatrix} \\
A &= (d \circledast \varphi) \\
Q &= \mu^{trans}(d \circledast \varphi)
\end{aligned}
\tag{12}
$$

3.3. Improvised feature learning

In this section we design the improvised version of CAE by introducing the dual frame; from (12) dual frame can be mathematically formulated as (13):

$$\ddot{Y} = \frac{1}{(I\_M + \mu^{trans}\mu)} [I\_M\ \mu] \tag{13}$$

hence considering the matrix inversion for average feeling dual frame CAE can be given as (14).

$$\ddot{Y} = \left[I - \frac{\mu^{trans}\mu}{2} \left(\frac{\mu}{2} \right) \right] \tag{14}$$

In given framelet coefficient W, reconstruction is given through the (15); the (15) represents network model of ICAE.

$$\dot{A} = A + 0.5(Q - \mu^{trans}A) \tag{15}$$

Further in (15), S indicates unspooling and $(Q - \mu^{trans}A)$ indicates residual.

3.4. Training of CNN

Moreover, segmentation process is affected through edge of the region, further disadvantage of basic model is duplicate information for features, and it fails to estimate the global feature for high resolution. Input d^{k+1} without convolution in given layer the problem definition can be represented through (16).

$$n^{j+1} = a^{j-1} \oplus S(\eth^k) \tag{16}$$

In (16), $\oplus$ integrates two images i.e., before applying the operator and after applying the operator; d^{k+1} represents the duplicated information. In improvised convolutional auto encoder (ICAE), network uses the remaining path for ignoring the duplicate for local feature map. In here remaining path is given right after pooling. Hence global feature map is passed through skip connections, also to assess the filter performance, performance rate is formulated. In the (17) feature map before the path and after the path is considered.

$$\text{Measuring rate} = \begin{cases} \text{if } feature\_map_z(v,w) < 0.01 & -0.5, \\ \text{otherwise,} & \dfrac{\Sigma_{v,w \in \text{object}} label(v,w) feature\_map_z(v,w)}{\Sigma_{v,w \in \text{object}} label(w,z) feature\_map_z(v,w)}, \end{cases} \tag{17}$$

Further in proposed model of convolutional auto encoder, up sampling is performed through introducing the deconvolution layer in the designed path and designed operation. Hence a_s^{j+1} represents the after-sampling signal and a_q^{j+1} represents the signal after convolutional layer and represented through (18).

$$a_s^{j+1} = \dot{A}_s^{j+1}(B(a^{l-1}); \delta_s^{j+1})$$
$$a_q^{j+1} \equiv A_q^{j+1}(a^{j-1} - a_s^{j+1}; \delta_s^{j+1}), \tag{18}$$

Similarly, $a_{s,t}^{j+1}$ indicates the deconvolution with vth kernel and weights; in here parameter set is combined with $(j+1)th$ layers and $a_{q,r}^{j+1}$ Indicates the rth kernel with r bias.

$$a_{s,t}^{j+1} = \eth\left(u_{v,u}^{j+1} \otimes^R B(a^{j-1}) + z_{v,u}^{j+1}\right) \in d_v^{k+1}$$
$$a_{q,r}^{j+1} = \eth\left(x_{q,r}^{j+1} \otimes (a^{j-1} - a_t^{k+1}) + z_{q,r}^{j+1}\right) \in a_q^{j+1}, \tag{19}$$

Further n_{ICAE}^{j+1} is considered as the ICAE convolutional operation in given $(j+1)$ layer on decoder; mathematical formulation is represented through (20).

$$n_{ICAE}^{j+1} = a_q^{j+1} \oplus S(a^j) \tag{20}$$

In the (20), feature information in given path is filtered through $a^{j-1} - a_s^{j+1}$. At last, we consider the global feature and local feature for absolute segmentation; feature for global information is represented through (21) and (22).

$$n_{ICAE}^{j+1} = S\left(A^j\left(B(a^{j-1})\right)\right) \oplus A_q^{j+1}\left(a^{j-1} - a_{low}^{j-1}; \tau_q^{j+1}\right) \tag{21}$$

$$n_{ICAE}^{j+1} = S\left(A^j\left(B(a^{j-1}); \tau_q^{j+1}\right)\right) \oplus \mathcal{E}_t^{n+1}\left(e^{n-1}; \tau_t^{n+1}\right) \tag{22}$$

3.5. Training of CNN

Moreover, due to the complexity of ICAE, proposed model has an issue of convergence speed and the training is quite complex; hence batch normalization layer is deployed for increasing the learning rate. In general batch normalization computes the standard and mean deviation for the previous layer, later it subtracts the mean and further divides through SD. This in terms makes ICAE converge faster, and it becomes marginally less sensitive to the input distribution and becomes further robust to distribution change for the longer term. Let's consider a layer with $c - dimensional$ input $V = \left(v^{(1)} \ldots \ldots v^{(c)}\right)$ then first we find the normalization of each dimension through (23).

$$\dot{v}^{(i)} = \left(v^{(i)} - C[v^{(i)}]\right)\left(Var[v^{(i)}]\right)^{-1/2} \tag{23}$$

Further we consider the batch Z of size k and normalization is applied to each activation independently and this can be given as (24):

$$Z = \{v_{1.........k}\} \tag{24}$$

after normalizing the values, we consider the linear transformation, and it is given through (25).

$$batch_{norm}: v_{1.........k} \rightarrow w_{1.........k} \tag{25}$$

Moreover, the batch normalization transformation is added to the network for higher learning rate i.e., manipulating the activation and thus increase the higher learning rate.

4. RESULTS AND DISCUSSIONS
4.1. Dataset description, training, and testing time
In any machine learning based algorithm dataset plays a major role as data require for model training needs to be sufficient enough to perform the model. In here we have used standard dataset from the open access digital database of thyroid ultrasound images from the Universidad Nacional de Colombia Laboratory [24]. Further this dataset is utilized for computation of proposed model. Moreover dataset comprises 92 images of thyroid ultrasound, out of theses 42 were from female and 50 from male from different age group. Moreover these images were captured through TOSHIBA linear transducer and extracted from ultrasound video sequence. These thyroid nodules images are stored in ultrasonography model which includes whole diagnostic description and annotation of thyroid lesions. Further these are carried out under supervision of two radiologist expert using the TI-RADS lexicon. To train the model it took 1070 seconds considering 32 optimization epochs. On the other side the existing segmentation model [20], [29] takes about 103.86 hour considering 20 optimization epochs. Thus, proposed segmentation model are much faster. The time taken for testing is 0.85 seconds for proposed and 3.25 seconds for existing segmentation model [20], [29].

4.2. Pictorial comparison description
Here pictorial representation of segmentation outcome achieved using different methodology is shown in Figure 2. The Figure 2 is composed original ultrasound image of thyroid nodule. Then, followed by ground truth image of thyroid nodule. Then, segmentation outcome achieved using existing method namely SSHOS is shown. Finally, the segmentation outcome achieved using proposed namely ICAE is given. From result achieved in Figure 2, it can be seen ICAE achieves better segmentation outcome in comparison with SSHOS method.
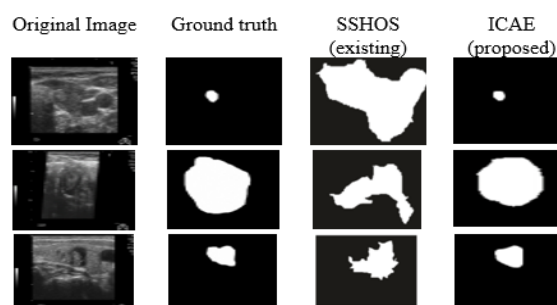

Figure 2. Segmentation outcome achieved using different methods

4.3. Metrics computation
Further to evaluate the model various metrics are considered and compared with existing methodology. The existing methodology have produced the genuine effort for segmentation of thyroid gland for thyroid cancer detection. These method includes self-organizing map (SOM) [25], abnormal region gradient magnitude (ARGM) [26], neutrosophic l-means (NLM) [27], neutrosophic distance regularized level set (NDRLS) [28] and existing model seed selection based on higher order spectra (SSHOS) [29]. The Jaccard Coefficient and Dice similarity coefficient is metrics used validating the existing and proposed segmentation outcomes.

4.4. Jaccard coefficient

A jaccard coefficient is used for measuring similarity and diversity among given image sets. Precisely, jaccard coefficient is calculated as the ratio of true positive predicted with respect to true positive, false positive and false negative values. Furthermore Figure 3 presents the comparison of various methodology with proposed model. In here SOM performs very badly with jaccard coefficient of 49.99; however other method like ARGM, NLM, and NDRLS achieves better jaccard coefficient of 90.45, 91.56, and 94.2, respectively. Further existing model i.e., SSHOS achieves better result with jaccard coefficient of 95.99 whereas ICAE achieves TPR of 99.18.

4.5. Dice similarity coefficient

In segmentation, Dice similarity Coefficient is an evaluation metric which is used for gauging the similarity between two given image. In general Dice similarity coefficient is ratio of 2* area of overlap (AoO) to total number of pixels in given images. Figure 4 represents comparison with various model in terms of dice similarity coefficient. State of art technique like SOM achieves 60.45% which is marginally less for application, improvising these ARGM, NLM and NDRLS achieves 78.45%, 91.09%, and 89.98% whereas existing model achieves 91.06%. Moreover NLM and NLM performs very well; however in comparison, proposed model achieves better than any of these model with 96.87%.
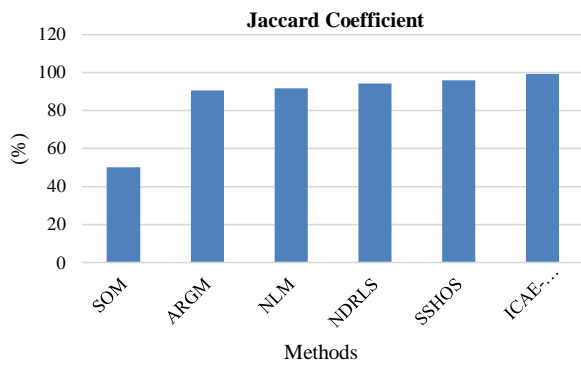

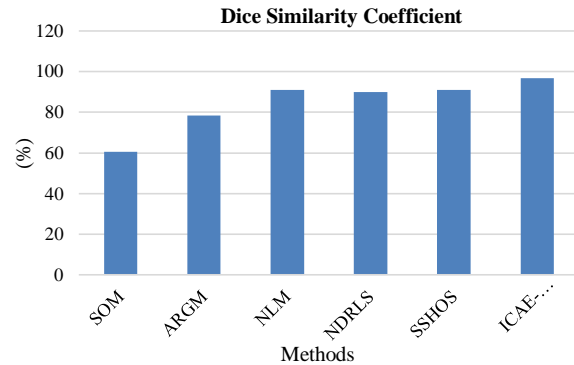Figure 3. Jaccard coefficient outcome achieved using different methods

Figure 4. Dice similarity coefficient outcome achieved using different methods

4.6. Accuracy and comparative analysis

Accuracy is one of the important performance metric measures in classification process; accuracy presents the correctly predicted model, further it is defined as ratio of number of samples correctly predicted to the total number of samples. The accuracy measured through correct prediction CP with respect to total number of samples TS which shows the proposd model achieves the accuracy of 98.39%. Further, we analyze the comparison of existing and proposed method by varying the performance metrics as shown in Table 1 and it is observed that in case of jaccard coefficient metrics, proposed mechanism achieves 49.19%, 8.73%, 7.62%, and 4.98% better than SOM, ARGM, NLM, and NDRLS mechanism respectively; further it also outperforms the existing approach with achieving 3.19% more efficient than the existing model. Furthermore, considering dice similarity Coefficient false positive rate; proposed mechanism outperforms the existing models by 36.42%, 18.42%, 5.78%, and 6.89% for SOM, ARGM, NLM, and NDRLS mechanism respectively, also it performs 5.81% better than the existing approach.

Table 1. Comparative analysis

Model	Jaccard Coefficient	Dice Similarity Coefficient
SOM [25]	49.99	60.45
ARGM [26]	90.45	78.45
NLM [27]	91.56	91.09
NDRLS [28]	94.2	89.98
SSHOS [29]	95.99	91.06
ICAE-Proposed	99.18	96.87

5.   CONCLUSION

Segmentation is considered as one of the eminent step in detection of thyroid cancer, in this research work improvised version of convolutional autoencoder, also known as ICAE is developed to achieve the absolute segmentation. ICAE is designed to overcome the shortcoming of traditional convolutional auto encoder and focuses on enhancing the image, better feature learning and achieving high learning rate. Moreover ICAE considers the traditional convolutional auto encoder and adds the skip connection to enhance the image information, introduce the dual frame to better feature learning and optimizes for higher learning rate. Moreover while evaluating the model through comparative analysis we observe that proposed ICAE outperforms various model including the existing model; furthermore ICAE achieves comparatively better results by 3.19% and 5.81% in terms of Jaccard coefficient and dice coefficient respectively. Segmentation has been always a difficult task in identification of disease through image as even slight changes in evaluation produces marginal difference; since considering the vulnerabilities of medical image analysis our model performs better, however there are several research area that needs to be considered and further optimization can be achieved in future. Future work would further consider adding different noise such as Gaussian, speckle and study the impact of segmentation outcome using ICAE and other existing models.

REFERENCES

[1]   K. B.-Domingo *et al.*, "Screening for thyroid cancer: US preventive services task force recommendation statement," *JAMA - Journal of the American Medical Association*, vol. 317, no. 18, pp. 1882–1887, May 2017, doi: 10.1001/jama.2017.4011.
[2]   M. P. J. Vanderpump, "The epidemiology of thyroid disease," *British Medical Bulletin*, vol. 99, no. 1, pp. 39–51, Sep. 2011, doi: 10.1093/bmb/ldr030.
[3]   M. N. Rachmatullah, S. Nurmaini, A. I. Sapitri, A. Darmawahyuni, B. Tutuko, and Firdaus, "Convolutional neural network for semantic segmentation of fetal echocardiography based on four-chamber view," *Bulletin of Electrical Engineering and Informatics*, vol. 10, no. 4, pp. 1987–1996, Aug. 2021, doi: 10.11591/EEI.V10I4.3060.
[4]   M. N. Farhan, M. G. Ayoub, H. M. Qassim, and A. K. Eesee, "Qualitative assessment of image enhancement algorithms for mammograms based on minimum EDV," *Telkomnika (Telecommunication Computing Electronics and Control)*, vol. 18, no. 2, pp. 928–935, Apr. 2020, doi: 10.12928/TELKOMNIKA.V18I2.14085.
[5]   C. Y. Chang, Y. F. Lei, C. H. Tseng, and S. R. Shih, "Thyroid segmentation and volume estimation in ultrasound images," *IEEE Transactions on Biomedical Engineering*, vol. 57, no. 6, pp. 1348–1357, Jun. 2010, doi: 10.1109/TBME.2010.2041003.
[6]   S. B. Kutty, R. W. O. K. Rahmat, S. S. Kassim, H. Madzin, and H. Hamdan, "An algorithm to measure unsymmetrical circle shape of intravascular ultrasound image using image processing techniques," *Bulletin of Electrical Engineering and Informatics*, vol. 10, no. 1, pp. 508–515, Feb. 2021, doi: 10.11591/eei.v10i1.2694.
[7]   D. K. Iakovidis, M. A. Savelonas, S. A. Karkanis, and D. E. Maroulis, "A genetically optimized level set approach to segmentation of thyroid ultrasound images," *Applied Intelligence*, vol. 27, no. 3, pp. 193–203, Jun. 2007, doi: 10.1007/s10489-007-0066-y.
[8]   N. Singh and A. Jindal, "A segmentation method and comparison of classification methods for thyroid ultrasound images," *International Journal of Computer Applications*, vol. 50, no. 11, pp. 43–49, Jul. 2012, doi: 10.5120/7818-1115.
[9]   N. H. Mahmood and A. H. Rusli, "Segmentation and area measurement for thyroid ultrasound image," *International Journal of Scientific & Engineering Research*, vol. 2, no. 12, pp. 1–8, 2011, Accessed: Feb. 06, 2022. [Online]. Available: http://www.ijser.org
[10]   K. B. Kim and D. H. Song, "Fully automatic segmentation of intima/adventitia of the vessel using Bezier curve from intravascular ultrasound," *International Journal of Electrical and Computer Engineering*, vol. 11, no. 3, pp. 2640–2646, Jun. 2021, doi: 10.11591/ijece.v11i3.pp2640-2646.
[11]   H. A. Nugroho, A. Nugroho, and L. Choridah, "Thyroid nodule segmentation using active contour bilateral filtering on ultrasound images," in *14th International Conference on QiR (Quality in Research), QiR 2015 - In conjunction with 4th Asian Symposium on Material Processing, ASMP 2015 and International Conference in Saving Energy in Refrigeration and Air Conditioning, ICSERA 2015*, Aug. 2016, pp. 43–46, doi: 10.1109/QiR.2015.7374892.
[12]   D. Selvathi and V. S. Sharnitha, "Thyroid classification and segmentation in ultrasound images using machine learning algorithms," in *2011-International Conference on Signal Processing, Communication, Computing and Networking Technologies, ICSCCN-2011*, Jul. 2011, pp. 836–841, doi: 10.1109/ICSCCN.2011.6024666.
[13]   P. Poudel, A. Illanes, D. Sheet, and M. Friebe, "Evaluation of commonly used algorithms for thyroid ultrasound images segmentation and improvement using machine learning approaches," *Journal of Healthcare Engineering*, vol. 2018, pp. 1–13, Sep. 2018, doi: 10.1155/2018/8087624.
[14]   V. Kumar *et al.*, "Automated and real-time segmentation of suspicious breast masses using convolutional neural network," *PLoS ONE*, vol. 13, no. 5, p. e0195816, May 2018, doi: 10.1371/journal.pone.0195816.
[15]   F. Milletari *et al.*, "Hough-CNN: Deep learning for segmentation of deep brain regions in MRI and ultrasound," *Computer Vision and Image Understanding*, vol. 164, pp. 92–102, Nov. 2017, doi: 10.1016/j.cviu.2017.04.002.
[16]   J. Yang, L. Tong, M. Faraji, and A. Basu, "IVUS-Net: An intravascular ultrasound segmentation network," in *Lecture Notes in Computer Science (including subseries Lecture Notes in Artificial Intelligence and Lecture Notes in Bioinformatics)*, vol. 11010 LNCS, Springer International Publishing, 2018, pp. 367–377.
[17]   C. Azzopardi, Y. A. Hicks, and K. P. Camilleri, "Automatic carotid ultrasound segmentation using deep convolutional neural networks and phase congruency maps," in *Proceedings - International Symposium on Biomedical Imaging*, Apr. 2017, pp. 624–628, doi: 10.1109/ISBI.2017.7950598.
[18]   P. Looney *et al.*, "Automatic 3D ultrasound segmentation of the first trimester placenta using deep learning," in *Proceedings - International Symposium on Biomedical Imaging*, Apr. 2017, pp. 279–282, doi: 10.1109/ISBI.2017.7950519.
[19]   J. Zhou, "Thyroid tumor ultrasound image segmentation based on improved graph cut," in *Proceedings - 2016 International Conference on Intelligent Transportation, Big Data and Smart City, ICITBS 2016*, Dec. 2017, pp. 130–133, doi: 10.1109/ICITBS.2016.72.

[20] J. Ma, F. Wu, T. Jiang, Q. Zhao, and D. Kong, "Ultrasound image-based thyroid nodule automatic segmentation using convolutional neural networks," *International Journal of Computer Assisted Radiology and Surgery*, vol. 12, no. 11, pp. 1895–1910, Jul. 2017, doi: 10.1007/s11548-017-1649-7.

[21] X. Ying *et al.*, "Thyroid nodule segmentation in ultrasound images based on cascaded convolutional neural network," in *Lecture Notes in Computer Science (including subseries Lecture Notes in Artificial Intelligence and Lecture Notes in Bioinformatics)*, vol. 11306 LNCS, Springer International Publishing, 2018, pp. 373–384.

[22] R. Yu *et al.*, "Localization of thyroid nodules in ultrasonic images," in *Lecture Notes in Computer Science (including subseries Lecture Notes in Artificial Intelligence and Lecture Notes in Bioinformatics)*, vol. 10874 LNCS, Springer International Publishing, 2018, pp. 635–646.

[23] K. Simonyan and A. Zisserman, "Very deep convolutional networks for large-scale image recognition," *3rd International Conference on Learning Representations, ICLR 2015-Conference Track Proceedings*, Sep. 2015, Accessed: Feb. 06, 2022. [Online]. Available: https://arxiv.org/abs/1409.1556v6

[24] N. Shrivastava and J. Bharti, "Automatic Seeded Region Growing Image Segmentation for Medical Image Segmentation: A Brief Review," *International Journal of Image and Graphics*, vol. 20, pp. 2050018, 2020, doi: 10.1142/S0219467820500187.

[25] M. M. Abdelsamea, G. Gnecco, and M. M. Gaber, "A SOM-based Chan-Vese model for unsupervised image segmentation," *Soft Computing*, vol. 21, no. 8, pp. 2047–2067, Oct. 2017, doi: 10.1007/s00500-015-1906-z.

[26] J. Shan, H. D. Cheng, and Y. Wang, "A novel segmentation method for breast ultrasound images based on neutrosophic l-means clustering," *Medical Physics*, vol. 39, no. 9, pp. 5669–5682, Aug. 2012, doi: 10.1118/1.4747271.

[27] D. Koundal, S. Gupta, and S. Singh, "Computer aided thyroid nodule detection system using medical ultrasound images," *Biomedical Signal Processing and Control*, vol. 40, pp. 117–130, Feb. 2018, doi: 10.1016/j.bspc.2017.08.025.

[28] S. O. Haji and R. Z. Yousif, "A novel neutrosophic method for automatic seed point selection in thyroid nodule images," *BioMed Research International*, vol. 2019, pp. 1–14, Apr. 2019, doi: 10.1155/2019/7632308.

[29] M. Böhland *et al.*, "Machine learning methods for automated classification of tumors with papillary thyroid carcinoma-like nuclei: A quantitative analysis," *PLoS ONE*, vol. 16, no. 9 September, p. e0257635, Sep. 2021, doi: 10.1371/journal.pone.0257635.

[30] Y. Guo *et al.*, "Classification and diagnosis of residual thyroid tissue in SPECT images based on fine-tuning deep convolutional neural network," *Frontiers in Oncology*, vol. 11, Oct. 2021, doi: 10.3389/fonc.2021.762643.

[31] G. R. Kim, E. Lee, H. R. Kim, J. H. Yoon, V. Y. Park, and J. Y. Kwak, "Convolutional neural network to stratify the malignancy risk of Thyroid nodules: Diagnostic performance compared with the American college of radiology Thyroid imaging reporting and data system implemented by experienced radiologists," *American Journal of Neuroradiology*, vol. 42, no. 8, pp. 1513–1519, May 2021, doi: 10.3174/ajnr.A7149.

[32] W. Li, S. Cheng, K. Qian, K. Yue, and H. Liu, "Automatic recognition and classification system of thyroid nodules in CT images based on CNN," *Computational Intelligence and Neuroscience*, vol. 2021, pp. 1–11, May 2021, doi: 10.1155/2021/5540186.

[33] J. Koh *et al.*, "Diagnosis of thyroid nodules on ultrasonography by a deep convolutional neural network," *Scientific Reports*, vol. 10, no. 1, Sep. 2020, doi: 10.1038/s41598-020-72270-6.

[34] F. Abdolali *et al.*, "A systematic review on the role of artificial intelligence in sonographic diagnosis of thyroid cancer: Past, present and future," *Frontiers in Biomedical Technologies*, vol. 7, no. 4, pp. 266–280, Feb. 2020, doi: 10.18502/fbt.v7i4.5324.

BIOGRAPHIES OF AUTHORS

Drakshaveni Gunjali ⓘ 🔗 SC Ⓟ is currently working as an Assistant Professor in the Department of Master of Computer Applications (MCA) at B M S Institute of Technology, Yelahanka, and Bangalore. She took second place in her M.tech. She is pursuing her PhD from Visvesvaraya Technological University (VTU), Belagavi, India. She has more than 18 years of experience in Teaching. She also worked in M S Ramaiah college for 5year. She is appointed as the member of BoE, VTU, and Belagavi. She has published papers in both National, International journals. She received Best Paper Incentive from BMSIT&M on 26.11.2020 for the paper titled "ultrasound and thermal image enhancement technique using convolution neural network". She was a reviewer for Sixth International Conference on "Emerging Research in Computing, information, communication and applications" (ERRICA-2020 held during September 25.9.2020 to 28.9.2020 at NMIT, Bangalore, India. Her major research areas are Medical Image Processing, Data Base Management, and Software testing. She can be contacted at email: gdrakshaveni23@gmail.com.

Dr. Prasad Naik Hamsavath ⓘ 🔗 SC Ⓟ is currently working as a Professor and Head of the Department of Master of Computer Applications (MCA) at Nitte Meenakshi Institute of Technology, Yelahanka, and Bangalore. He has PhD from Jawaharlal Nehru University (JNU), New Delhi, India. He has served as Assistant Director in Software Technology Parks of India (STPI), Ministry of Communication and Information Technology (MC&IT), New Delhi, Government of India and received the Best Employee award by then Director-STPI-Noida. He also served as 'Software Engineer' at Calance Software Pvt Ltd, Gurgaon, and Haryana and later he served in Educational Consultants India Limited (EdCIL), Ministry of human resource and development (MHRD), New Delhi, Govt. of India. He has authored 03 books and more than 15 books are edited by him on different emerging areas. His major research areas are Mobile Ad-hoc wireless networks, information systems, computer networks, cloud computing, internet of things (IoT). He has received a prestigious award "Dr. Abdul Kalam Lifetime Achievement Award" in the field of Teaching/Training/Research/Administration and also received "Young Faculty" award at 2nd Academic Brilliance Awards from Education Expo TV, New Delhi. He has lifetime membership of ISTE, MCSI and ACEEE. He can be contacted at email: hod-mca@nmit.ac.in.